APPENDIX.—NOTATION

The following symbols are used in this paper:

A_r = reduced force matrix (Eq. 46b);
C_d = connection matrix for displacement (Eq. 14);
C_f = connection matrix for force (Eqs. 4, 43, and 52);
D_r = displacement-matrix (Eq. 8 and Figs. 2);
F_r = force matrix (Eq. 1 and Figs. 2);
f_{ri} = axial force in members of r^{th} unit [Fig. 2(a)];
f_r' = hyperstatic axial force (Figs. 2);
i = 1, 2, 3, 4; Fig. 2(a);
K_r = column matrix defined in Eqs. 28b, and 31b;
k_r = flexibility of hyperstatic member (Eq. 17);
k_r = flexibility matrix (Eq. 12a);
L = shift operator for force-matrix (Eq. 6a);
M = 4-by-1 operational matrix defined in Eq. 6b;
N = shift operator (Eq. 19);
n = number of bays (Fig. 1);
P_r = load matrix (Eq. 2 and Figs. 2);
P = magnitude of some standard load (Eq. 28a);
P_r, Q_r, P_r', Q_r' = components of nodal loads (Fig. 1);
Q = consolidated shift operator (Eq. 23a);
R = reduction matrix (Eq. 46c);
r = 0, 1, 2,...., n+1 (Fig. 1);
T = shift operator for displacement matrix (Eq. 16a);
U = feed operator for force matrix (Eq. 6c);
U_r, U_r' = node displacements (Eqs. 7 and Figs. 2);
u_r, v_r, u_r', v_r' = components of node displacements [Fig. 2(a)];
V = shift operator for displacement-matrix (Eq. 16b);
W = consolidated feed operator (Eq. 23b);
Z_r = eigenmatrix (Eq. 21);
$\Delta l, \Delta l'$ = elongation of member (Eqs. 9 and 17);
Δ_r = elongation-matrix (Eq. 12b);
θ = inclination of diagonal member [Fig. 3(a)];
$\approx$ = equivalent equality (Eq. 26);
$\lfloor \quad \rfloor$ = row matrix; and
$\{ \quad \}$ = column matrix.

Journal of the
STRUCTURAL DIVISION
Proceedings of the American Society of Civil Engineers

TEST OF A FLAT SLAB REINFORCED WITH WELDED WIRE FABRIC

By James O. Jirsa,[1] A. M. ASCE, Mete A. Sozen,[2] M. ASCE, and Chester P. Siess,[3] F. ASCE

INTRODUCTION

The structure described in this paper was tested in the course of the "Investigation of Multiple-Panel Reinforced Concrete Floor Slabs"[4] conducted in the Structural Research Laboratory of the University of Illinois Civil Engineering Department. The nine-panel structure, designated F3, was reinforced with welded wire fabric. Test Structure F3 was one of a series of five quarter-scale models tested in this program and followed F1, a flat plate[5] and F2, a flat slab reinforced with intermediate grade reinforcement.[6]

Test structure F3 (Fig. 1) was planned as a representative flat slab reinforced with welded wire fabric, in accordance with the ACI Building

Note.—Discussion open until November 1, 1966. To extend the closing date one month, a written request must be filed with the Executive Secretary, ASCE. This paper is part of the copyrighted Journal of the Structural Division, Proceedings of the American Society of Civil Engineers, Vol. 92, No. ST3, June, 1966. Manuscript was submitted for review for possible publication on February 17, 1966.

[1] Asst. Prof. of Civ. Engrg., Rice Univ., Houston, Tex.
[2] Prof. of Civ. Engrg., Univ. of Illinois, Urbana, Ill.
[3] Prof. of Civ. Engrg., Univ. of Illinois, Urbana, Ill.

[4] Sozen, M. A., and Siess, C. P., "Investigation of Multiple-Panel Reinforced Concrete Floor Slabs; Design Methods—Their Evolution and Comparison," Journal of the American Concrete Institute, Vol. 60, No. 8, August, 1963, pp. 999-1027.

[5] Hatcher, D. S., Sozen, M. A., and Siess, C. P., "Test of A Reinforced Concrete Flat Plate," Journal of The Structural Division, ASCE, Vol. 91, No. ST5, Proc. Paper 4514, October, 1965, pp. 205-231.

[6] Hatcher, D. S., Sozen, M. A., and Siess, C. P., "A Study of Tests on A Flat Plate and A Flat Slab," Structural Research Series No. 217, Civil Engineering Studies, Univ. of Illinois, Urbana, Ill., July, 1961.

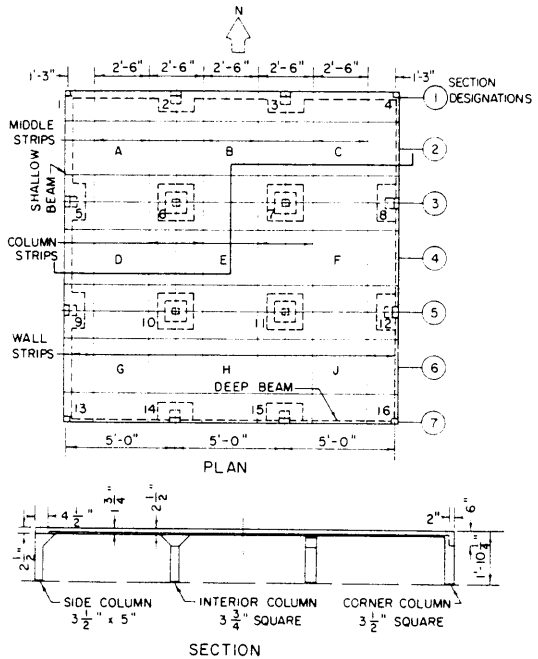

FIG. 1.—PLAN AND SECTION OF TEST STRUCTURE F3

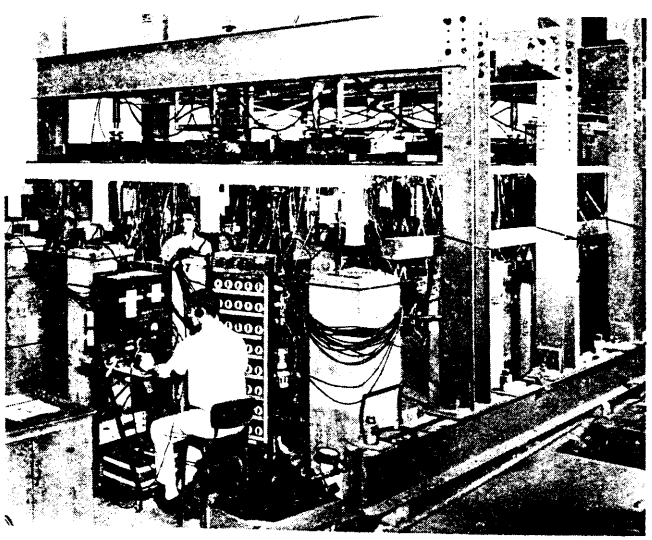

FIG. 2.—VIEW OF TEST STRUCTURE

Code (318-56).[7] Considerations related to the size of the test structure have been presented elsewhere.

DESCRIPTION OF THE TEST STRUCTURE

Design.—A prototype slab having 20-ft square panels was designed according to the "Empirical Design Method" specified in Section 1004 of ACI 318-56. The slab was designed for a live load of 200 psf and a dead load of 85 psf. The spandrel beams were designed to carry a wall load of 600 lb

TABLE 1.—AREA OF SLAB REINFORCEMENT AT DESIGN SECTIONS[a]

Section	Wall Strip		Middle Strip		Column Strip
	Adjacent to Shallow Beam	Adjacent to Deep Beam	Interior	Exterior	
1	0.200	0.122	0.135	0.135	0.303
2	0.141	0.080	0.228	0.238	0.262
3	0.215	0.140	0.184	0.184	0.429
4	0.122	0.080	0.182	0.192	0.231
5	0.215	0.140	0.184	0.184	0.429
6	0.141	0.080	0.228	0.238	0.262
7	0.221	0.091	0.231	0.231	0.231

a in square inches.

TABLE 2.—SECTIONAL AREAS OF WELDED WIRE FABRIC

Gage No.	Diameter, in inches	Area, in square inches
9.5	0.142	0.0157
10	0.135	0.0143
11.5	0.115	0.0102
12	0.106	0.0087
12.5	0.099	0.0076
13	0.092	0.0066
14	0.080	0.0050
14.5	0.077	0.0046
15	0.072	0.0041
16	0.063	0.0031

per ft. The working stresses were 1,350 psi for the concrete and 20,000 psi for the reinforcement. All details were in accordance with ACI 318-56.[7]

The dimensions of the prototype were scaled by a factor of 1/4 to obtain the dimensions of the test structure.

Dimensions.—A plan view and a profile section of the test structure are shown in Fig. 1. The structure had nine 5-ft square panels arranged three by three. The critical design sections and all geometrical properties are indicated in Fig. 1.

7 "Building Code Requirements for Reinforced Concrete (ACI 318-56)," ACI Committee 318, Journal of the American Concrete Institute, Detroit, Vol. 52, No. 9, May, 1956, pp. 913-986.

The columns in the test structure were pin-ended. The length of the columns was chosen to provide a stiffness comparable to that of the prototype structure columns which extended above the floor as well. A view of the test structure is shown in Fig. 2.

Reinforcement.—The slab reinforcement in the prototype consisted of 1/2-in. square bars. In the first test structure built using this prototype design,[5] a direct bar for bar substitution was made using 1/8-in. square bars. However, such a direct substitution was not practical for welded wire fabric. The wire size and spacing were obtained on the basis of steel area required per foot.

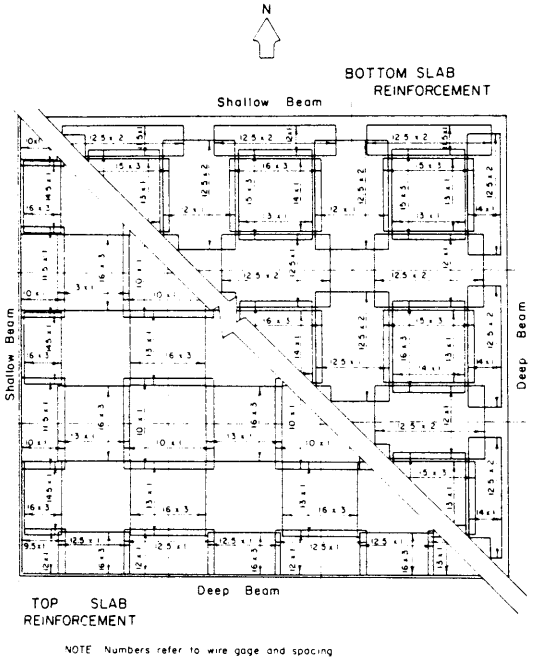

FIG. 3.—SLAB REINFORCEMENT

Information on slab reinforcement is given in Tables 1 and 2 and Fig. 3. The arrangement and sizes of beam and column reinforcement are shown in Figs. 4 and 5.

MATERIALS AND CONSTRUCTION

Reinforcing Steel.—The slab reinforcement consisted of specially manufactured small-scale welded wire fabric. A representative stress-strain curve for the wire is shown in Fig. 6. Three samples cut directly from the fabricated mats were used to obtain the stress-strain curves for each wire size.

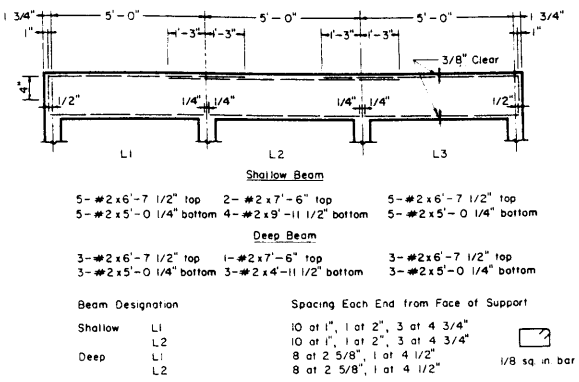

FIG. 4.—BEAM REINFORCEMENT

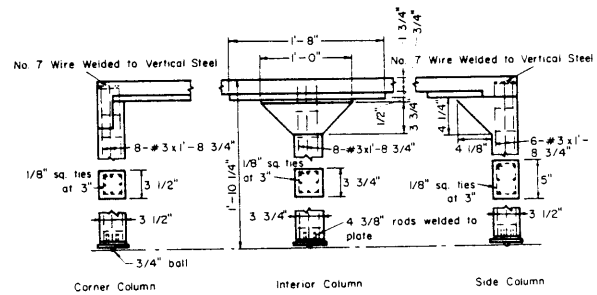

FIG. 5.—COLUMN REINFORCEMENT

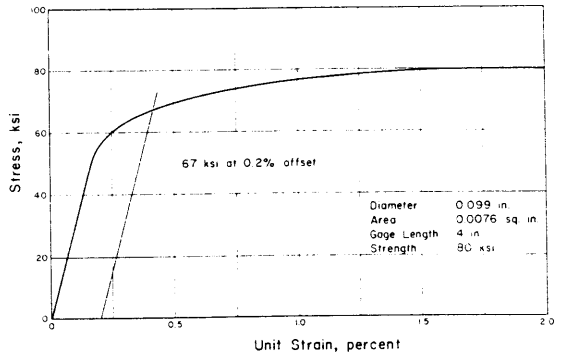

FIG. 6.—REPRESENTATIVE STRESS-STRAIN RELATIONSHIP FOR WELDED WIRE FABRIC

The unit strain at fracture measured over a 4-in. length including the zone of fracture ranged from 0.015 to 0.025. The initial modulus of elasticity was 30×10^6 psi. The ultimate stress ranged from 70,000-81,000 psi.

The wire mats were placed in a moist room for several days and allowed to rust. The mats were then wire brushed to remove the loose rust and improve the bond properties of the reinforcement.

The beams were reinforced with No. 2 deformed bars having an average yield stress of 54,000 psi. The columns were reinforced with No. 3 deformed bars with an average yield stress of 55,000 psi. The ties and stirrups were fabricated of 1/8-in. square plain bars with an average yield stress of 47,000 psi. The modulus of elasticity for all the beam and column steel was 30×10^6 psi.

Concrete.—A small-aggregate concrete composed of Type 1 portland cement, coarse sand, fine lake sand, and water was used. The aggregate comprised 80% Wabash River sand and 20% fine lake sand by weight. The aggregate/cement ratio was 4.9 and the water/cement ratio was 0.72. The structure was covered with wet burlap for seven days following casting.

TABLE 3

	Compressive strength	Modulus of rupture
56 days[a]	2x4 cyl. 3760 psi (St. Dev.=480 psi, 33 tests) 4x8 cyl. 3900 psi (St. Dev.=270 psi, 18 tests)	750 psi (12 tests)
100 days[b]	2x4 cyl. 3670 psi (St. Dev.=520 psi, 20 tests) 4x8 cyl. 3990 psi (St. Dev.=410 psi, 18 tests)	800 psi (12 tests)

[a] The initial modulus of elasticity of the concrete was 3.7×10^6 psi at 56 days.
[b] Measurements obtained at 100 days gave the same value.

The entire surface of the structure was then painted with "Traffic White" to reduce moisture loss.

The compressive strength of the concrete was determined using 2-in. by 4-in. and 4-in. by 8-in. cylinders. The modulus of rupture was obtained from 2-in. wide by 1 3/4-in. deep beams loaded at the third points of a 15-in. simple span. The concrete properties are summarized in Table 3.

TEST EQUIPMENT

The load was applied at sixteen symmetrically located points in each panel to simulate a uniform load. The columns were supported by dynamometers calibrated to measure the magnitude of the reaction.

A total of 350 electric resistance strain gages were used to measure strains. Of these, 320 were mounted on the reinforcement before casting. Deflections were measured at the centers of all panels and mid-points of all column center lines.

The loading system and instrumentation are described briefly by Hatcher[5] and in detail by Jirsa.[8]

TEST PROGRAM

Chronology.—Tests on structure F3 were made between April 20 and June 21, 1961. Tests 500 and 501 were at loads below the estimated cracking load. The structure was uniformly loaded to design load in Test 502. Tests 503 to 511 were at overload levels (1.5 LL + 1.0 DL) with 503 being a uniform load test and the remainder consisting of various pattern loadings. Tests 512 through 514 were the loadings to failure. Tests 502, 503, and 512 through 513 are reported herein.

Test Procedure.—Each test consisted of the application of a particular magnitude and pattern of load in one or more increments. Data were read and recorded after each increment. All electrical strain readings were taken semi-automatically and punched directly into IBM cards by an analog-to-decimal converter. Approximately 25 min were needed to complete the 449 electric readings during each load increment. Simultaneously, the deflection dials were read and the structure was inspected for cracks.

Data Reported.—The behavior of the structure is evaluated in terms of measurements of strains and deflections, and visual observations of cracking at various stages of loading. The response of the structure to uniform loading is considered for the following tests: (1) test 502, Design load, 286 psf; (2) test 503, Overload, 380 psf; and (3) tests 512 and 513, Failure.

In tests 504 through 511 pattern loadings were applied on the structure to produce maximum moments that are not directly considered herein. Loading to failure began during test 512 but at a maximum load of 674 psf the interior reaction dynamometers failed. After replacing the damaged dynamometers, loading was concluded in test 513.

The quantities examined in the following sections are cumulative and include dead load and residual effects. The load-deflection curves in Fig. 7 illustrate the method used to obtain these quantities. Curve E0, the midpanel deflection of the interior panel, is made up of two solid curves. The initial curve is for test 502. Tests 501 and 502 consisted of low levels of loading that created no measureable residual effects. The dead load (44 psf) deflection was obtained by extrapolation. The second solid line represents deflections measured in test 513 during loading to failure. The location of the origin of this portion of the curve is determined by the residual deflections accumulated during loading in tests 503 through 512. The broken line delineates the deflections that would have been measured if the structure had been loaded to failure in one continuous test.

BEHAVIOR AT DESIGN LOAD

The total load on the structure in test 502 was 286 psf corresponding to the design load of 285 psf. The maximum load was reached in four approximately equal increments.

8 Jirsa, J. O., Sozen, M. A., and Siess, C. P., "An Experimental Study of A Flat Slab Floor Reinforced with Welded Wire Fabric," Structural Research Series No. 249, Civil Engineering Studies, Univ. of Illinois, Urbana, Ill., June, 1962.

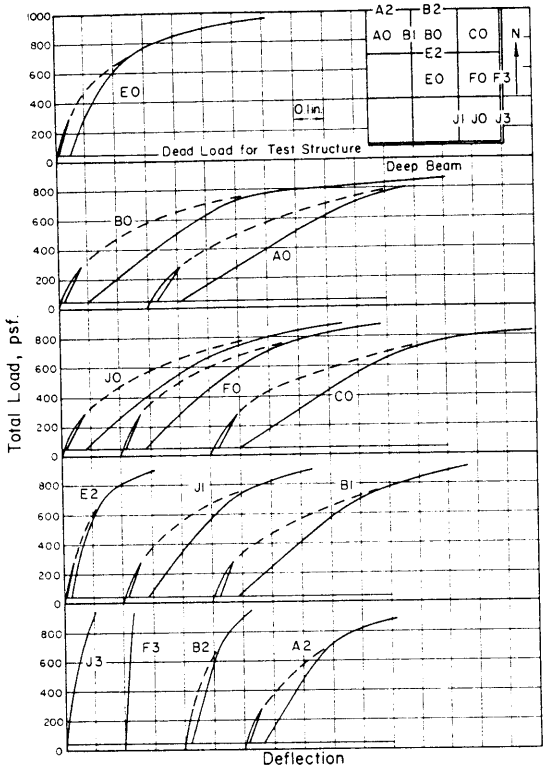

FIG. 7.—LOAD-DEFLECTION CURVES

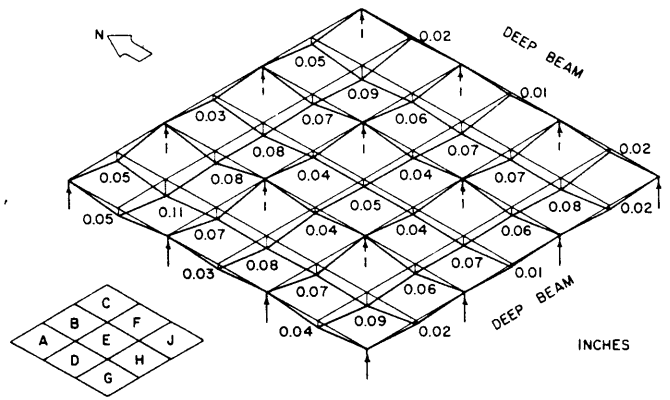

FIG. 8.—DEFLECTIONS AT DESIGN LOAD

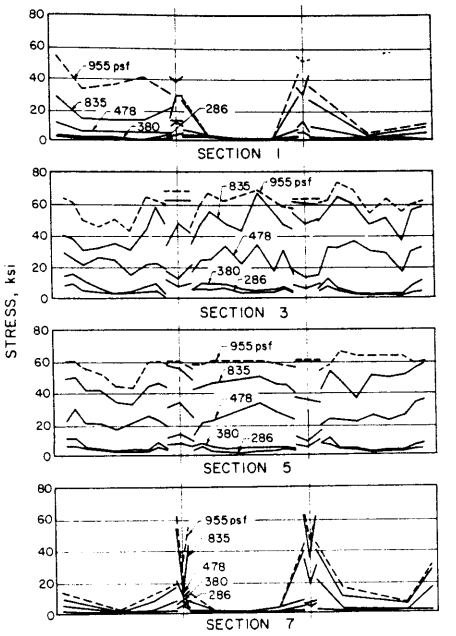

FIG. 9.—REINFORCEMENT STRESS DISTRIBUTION: NEGATIVE MOMENT SECTIONS

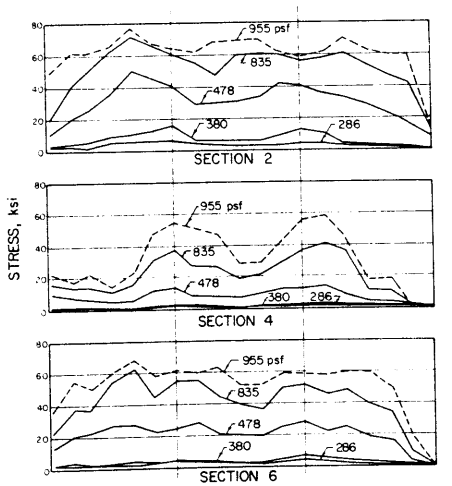

FIG. 10.—REINFORCEMENT STRESS DISTRIBUTION POSITIVE MOMENT SECTIONS

Deflections.—The load-deflection relationships measured during loading and unloading are shown in Fig. 7 by the initial solid part of each curve. The locations of measurements are shown in the upper right corner of Fig. 7.

The load-deflection curves measured in test 502 were nearly linear throughout the test although the curves for A0 and B1 exhibited a marked nonlinearity with ensuing residual effects. There were no residual deflections measured at F3 and J3 (deep beam deflections) after unloading. The load-deflection relationships indicate that the stiffness of the structure was practically unchanged after test 502.

The distribution of deflections at 286 psf is shown in Fig. 8. The maximum deflection was 0.11 in. measured in panel A, the corner panel bounded by shallow beams. This deflection corresponds to about L/550, in which L is the center-to-center distance between columns. The deflections in the rows of panels bounded by shallow beams (ABC, ADG) were slightly greater than those measured in panels bounded by deep beams (CFJ, GHJ).

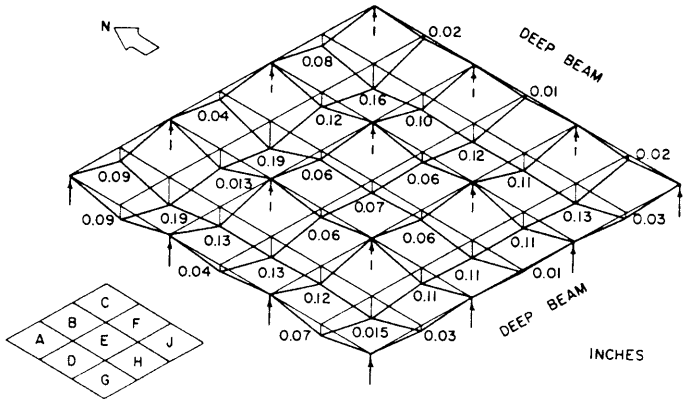

FIG. 11.—DEFLECTIONS AT 1.0DL + 1.5LL

Reinforcement Stresses.—The stresses for negative moment sections 1, 3, 5, and 7 are shown in Fig. 9 and those for the positive moment sections 2, 4, and 6 are shown in Fig. 10. The stress distributions are identified by the loads at which the measurements were taken. Stresses in the beam reinforcement and at the interior faces of the interior columns are not shown.

The stresses in test 502 were very small, less than 10 ksi at all sections except the exterior faces of the interior column capitals where this stress was exceeded slightly.

Cracking.—No cracks were found on the bottom of the slab (positive moment sections) and only a few very short cracks were found over one of the interior columns even though the load-strain curves implied cracking

in the column strips of negative moment sections 3 and 5.

BEHAVIOR IN TEST 503 (1.0DL+1.5LL)

The total load of 380 psf applied in test 503 was reached in four increments. This was the first test in which the structure was loaded beyond the design load.

Deflections.—The distribution of deflections at 380 psf is shown in Fig. 11. The maximum deflection was 0.19 in. at the centers of panels A and B. This is a deflection of slighly less than L/300 which is still low in view of the load magnitude. The deflections over the entire structure, except the deep beam and interior panel deflections, were approximately 50% greater than the deflections at 286 psf, whereas the load increased 35% from test 502 to 503. At 380 psf, the greater deflections in the panels adjacent to the shallow beams were quite apparent.

Reinforcement Stresses.—The stress distributions at 380 psf are shown in Figs. 9 and 10. The negative moment stresses across sections 3 and 5 and positive moment section 2 showed the greatest increases at 380 psf. The relative increases were particularly large at the faces of the interior columns.

The stresses in test 503 were below 15 ksi across the negative moment sections except at the interior column faces where they reached 20 ksi. The positive moment stresses were less than 10 ksi in sections 4 and 6 and somewhat greater in section 2.

Cracking.—The crack patterns on the top and bottom of the slab are shown in Figs. 12 and 13. Bottom cracks were observed for the first time in this test. Cracking was more pronounced on the bottoms of the panels adjacent to the shallow beams in keeping with the higher stresses and deflections in those panels.

The crack pattern on the top surface of the structure (Fig. 12) indicates that cracking had occurred over all the columns during the increase in load to 380 psf. However, the cracks on the top of the slab were short and were confined generally to the surface within the drop panels.

Flexural cracking was noted in the beams, the negative moments sections showing the most cracking. Cracks were observed in the exterior columns.

All existing cracks in the structure could be classified as hairline cracks: The maximum crack width did not exceed 0.005 in.

BEHAVIOR IN TEST TO FAILURE

Pattern loads were applied to the structure during tests 504 through 511 in which the load did not exceed 1.5 live load (LL) + 1.0 dead load (DL). These tests produced some additional cracking that was largely confined to short extensions of the existing cracks.

Loading to failure was begun in test 512 with the load on the structure reaching 674 psf (approximately 3 LL + 1.0 DL) when the interior reaction dynamometers failed. Because the loading system was relatively stiff, the load was reduced drastically after a small downward deflection of the slab had occurred. This decrease in load prevented serious damage to the structure and permitted loading to be continued after the supports had been replaced.

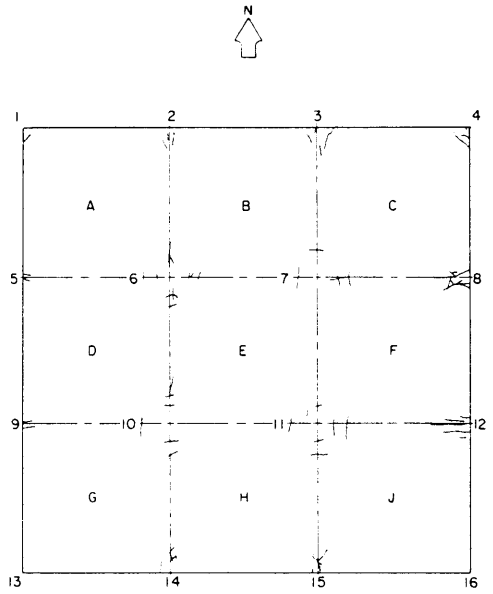

FIG. 12.—TOP CRACK PATTERN AT 1.0DL + 1.5LL

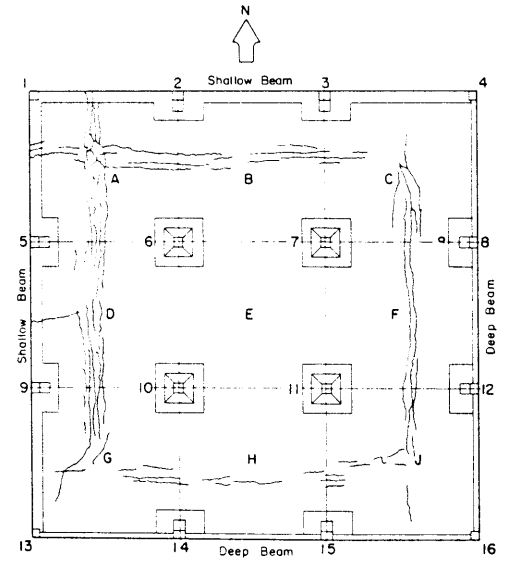

FIG. 13.—BOTTOM CRACK PATTERN AT 1.0DL + 1.5LL

In addition to replacing the damaged supports, the exterior beam-column connections were strengthened. A prestressing clamp was attached to the column to permit a direct transfer of moment from the slab to the column and to relieve some of the distress at the beam-column connection.

A maximum total load of 955 psf was attained in test 513. At this load, failure occurred in panels ABC. Additional loading was attempted on the remaining panels but failure was imminent in all but panel E. The load on Panel E was increased, with only a nominal load on the remainder of the panels. Failure of panel E occurred at a load of 1500 psf.

Deflections.—Representative load-deflection relationships for test 513 are shown in Fig. 7 by the second solid parts of the plotted curves. The initial slopes of these curves are considerably less than in test 502 indicating the effect of additional cracking. There was a marked increase in the rate of deflection at 800 psf, especially in panels ABC, which failed first. Although

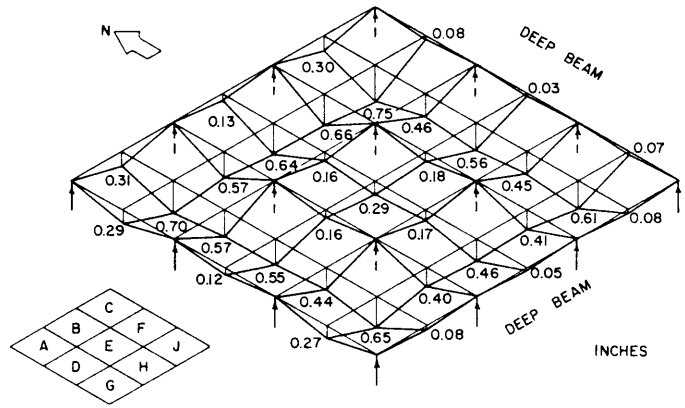

FIG. 14.—DEFLECTIONS AT 1.0DL + 3.4LL

the curves for the shallow beams exhibited a similar trend, the curves for the deep beams showed almost no change throughout the testing program.

The distribution of deflections at 764 psf (3.4 LL + 1.0 DL) is shown in Fig. 14. Fig. 14 illustrates the formation of a "trough" in panels ABC and ADG. The relatively small deflections of the interior panel and the deep beams with respect to the remainder of the structure is noteworthy.

Reinforcement Stresses.—The stresses increased rapidly after a level of 380 psf had been surpassed. The stresses at 478 psf were measured during the sequence of loading in test 513 and reflect the cracking that occurred in test 512 under a higher load. The stresses at 955 psf were obtained by projecting the load-strain curves.

The stresses across negative moment sections 3 and 5 (Fig. 9) at 955 psf were approximately 60 ksi almost uniformly along the section. The stresses across sections 1 and 7 were low except in the immediate vicinity of the columns. The exterior beam-column connections did not have sufficient

torsional stiffness and strength to develop high stresses across the beam faces.

The stresses across positive moment section 2 (Fig. 10) were higher than those across sections 4 and 6. The projected strains indicated that, at

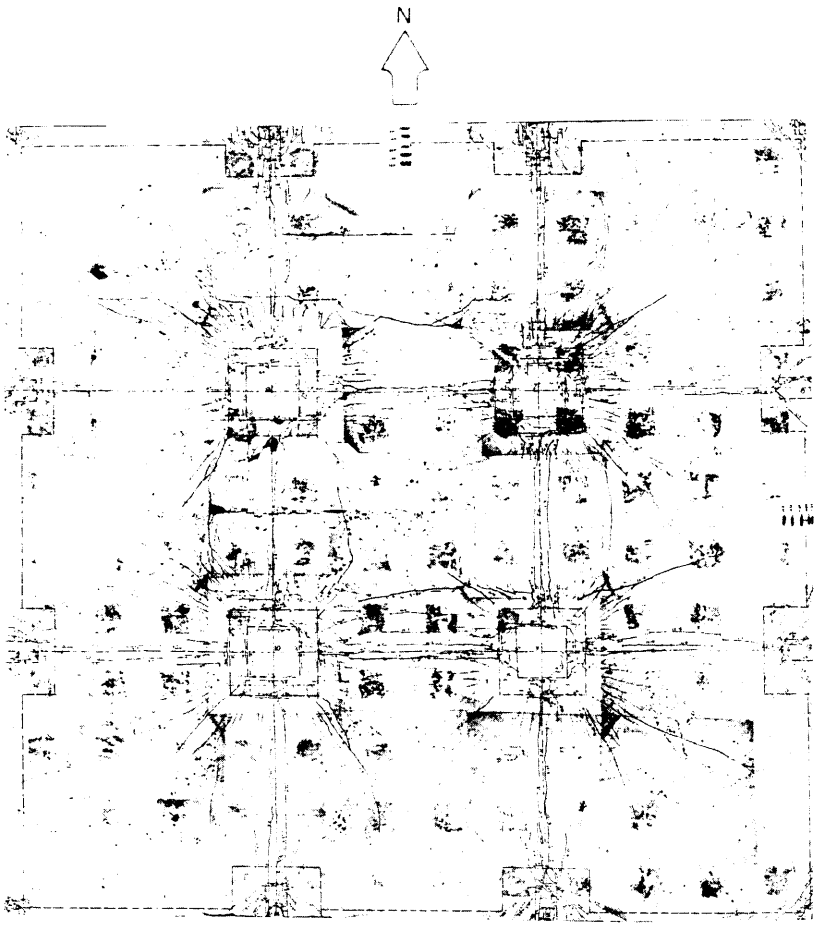

FIG. 15.—COMPOSITE PHOTOGRAPH OF TOP CRACK PATTERN AFTER TEST TO FAILURE

955 psf, fracture of the reinforcement was not distant. The location of highest strains corresponded to the location of the failure in panels A and B.

Cracking.—The crack patterns on the top and bottom of the structure following the test to failure are shown in Figs. 15 and 16. The darker lines indicate the cracks that were observed in the initial stages of loading. Generally, these had greater widths.

At 477 psf (test 512) the cracking on the bottom of the slab extended almost all along positive sections. In addition, a series of cracks formed which extended from the midpoint of the corner panels to the corner columns. Crack widths on the bottom of the slab were less than 0.005 in. Cracking on

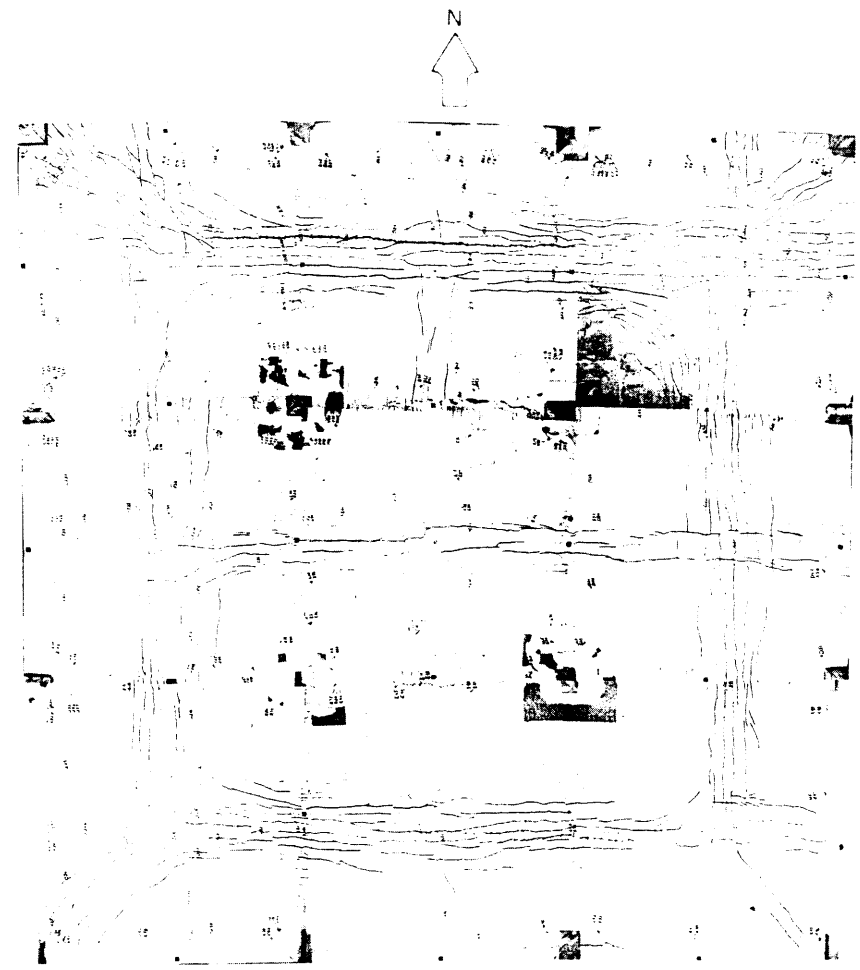

FIG. 16.—COMPOSITE PHOTOGRAPH OF BOTTOM CRACK PATTERN AFTER TEST TO FAILURE

the top surface of the slab was concentrated around the columns with cracks radiating from the columns in all directions. The measured crack widths were as large as 0.01 in., however, they averaged approximately 0.005 in.

Torsional cracking was noted in the beams at 477 psf. These cracks were most pronounced in the shallow beams. At 566 psf, these cracks widened and

considerable distress was noted at the beam-column connections. The application of the final load increment in test 512 (674 psf) resulted in severe rotations of the beam-column connections at columns 2 and 3 (Fig. 17.) The inability of the beam-column connections to transmit further moment contributed to the failure of the interior reaction dynamometers.

FIG. 17.—VIEWS OF BEAM-COLUMN CONNECTIONS

At 835 psf (test 513) different areas of distress became apparent, cracking was extensive over the interior columns and the cracks on the bottom of the structure at section 2 opened considerably. This corresponded to the high stresses and deflections measured in panels ABC at this load.

Failure.—As the load reached 955 psf, the structure failed with the collapse of panels ABC. The steel fractured for a distance of nearly 45 in. in panels A and B. The stresses, based on projections of load-strain curves, were approximately 80 ksi (ultimate stress) across section 2. The sudden destruction of the positive moment sections demanded large rotations at the exterior and interior columns leading to the complete collapse of one of the exterior columns.

Although failure was attributed to the collapse of panels A and B, careful inspection of the structure showed the positive moment sections bordering the other shallow beam and the two deep beams were extensively cracked and the cracks had widened during the final load increment. Furthermore, it was apparent that all the beam-column connections were severely damaged and were unable to transmit any increase in moment to the columns.

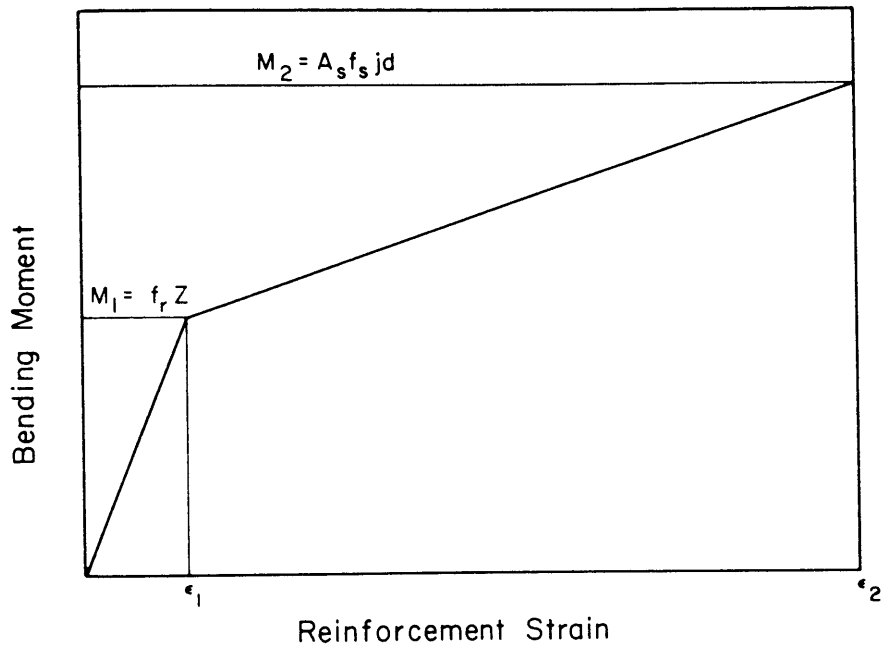

FIG. 18.—ASSUMED RELATIONSHIP BETWEEN BENDING MOMENT AND SLAB REINFORCEMENT STRAIN

It is of interest to note that the interior panel was not severely cracked at 955 psf. It was loaded to failure after the remainder of the structure could not sustain additional load. The load was approximately 1,500 psf when the panel was "pushed through" the structure. This final loading was responsible for a majority of the cracking in the interior panel shown in Figs. 15 and 16 and spalling of the interior-column drop panels, which can be seen in Fig. 16.

MEASURED BENDING MOMENTS

The bending moments at all design sections were calculated from measured steel strains using the idealized relationship shown in Fig. 18. The break in

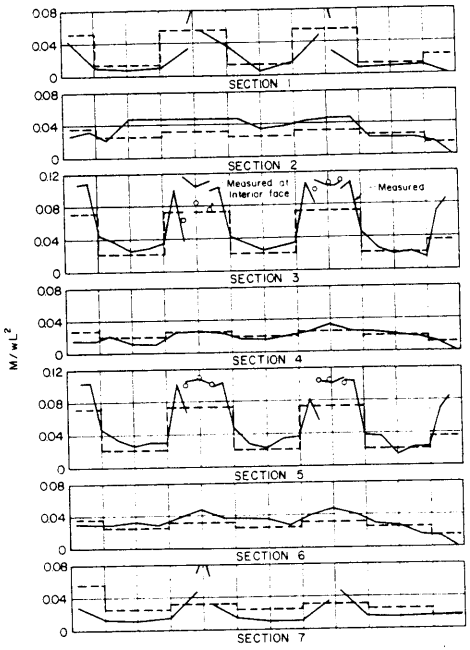

FIG. 19.—MEASURED AND DESIGN BENDING MOMENT COEFFICIENTS AT 1.0DL + 1.0LL

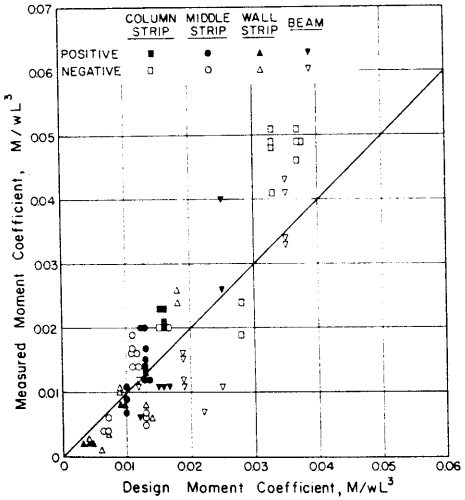

FIG. 20.—COMPARISON OF MEASURED AND DESIGN MOMENT COEFFICIENTS

TABLE 4.—MEASURED AND DESIGN MOMENT COEFFICIENTS FOR DESIGN STRIPS[a]

Section		Moment Coefficients, M/wL³							
		Beam (shallow)	Wall strip	Middle strip	Column strip	Middle strip	Column strip	Middle strip	Wall strip	Beam (deep)
1	Measured	0.012	0.008	0.004	0.024	0.006	0.019	0.004	0.001	0.007
	Design	0.012	0.013	0.007	0.028	0.007	0.028	0.007	0.006	0.022
2	Measured	0.011	0.008	0.020	0.023	0.020	0.023	0.012	0.002	0.026
	Design	0.016	0.009	0.013	0.016	0.013	0.016	0.013	0.004	0.025
3	Measured (Ext.)	0.015	0.024	0.019	0.046	0.017	0.049	0.014	0.011	0.041
	Measured (Int.)	0.012	0.024	0.019	0.041	0.017	0.048	0.014	0.011	0.034
	Design	0.019	0.018	0.011	0.037	0.011	0.037	0.011	0.009	0.035
4	Measured	0.006	0.004	0.007	0.013	0.009	0.014	0.011	0.002	0.011
	Design	0.012	0.007	0.010	0.013	0.010	0.013	0.010	0.003	0.017
5	Measured (Int.)	0.011	0.026	0.016	0.051	0.016	0.049	0.014	0.010	0.033
	Measured (Ext.)	0.016	0.026	0.016	0.051	0.016	0.049	0.014	0.010	0.043
	Design	0.019	0.018	0.011	0.037	0.011	0.037	0.011	0.009	0.035
6	Measured	0.011	0.008	0.015	0.020	0.017	0.021	0.012	0.002	0.040
	Design	0.016	0.009	0.013	0.016	0.013	0.016	0.013	0.004	0.025
7	Measured	0.011	0.006	0.006	0.020	0.005	0.020	0.007	0.002	0.001
	Design	0.012	0.014	0.013	0.016	0.013	0.016	0.013	0.004	0.025

the curve refers to cracking of the concrete and the terminal point to the proportional limit of the welded wire fabric or yield stress of the deformed bars. In determining the moments from strain measurements, the deep beams were assumed to act as L-beams with a flange width equal to the beam width plus four slab thicknesses and to be restrained from torsional rotation. The twisting moments between the supporting elements and the slab were ignored.

Moments were calculated using strain measurements taken at a load of 286 psf in test 502 (Design Load). Fig. 19 shows the distribution of slab unit moment across the critical sections and in Table 4 the moments across the various design sections are tabulated. The design moments are also shown.

TABLE 5

Source	Moments Across the Entire Structure		
	Adjacent to Shallow Beam Sections 1-2-3	Interior Sections 3-4-5	Adjacent to Deep Beam Sections 5-6-7
Calculated from strains	$0.305wL^3$	$0.300wL^3$	$0.311wL^3$
Calculated (Assumption 1)	$0.292wL^3$	$0.282wL^3$	$0.298wL^3$
Calculated (Assumption 2)	$0.289wL^3$	$0.280wL^3$	$0.312wL^3$

TABLE 6

Source	Moments in Interior Bay		
	Adjacent to Shallow Beam Sections 1-2-3	Interior Sections 3-4-5	Adjacent to Deep Beam Sections 5-6-7
Calculated from strains	$0.089wL^3$	$0.088wL^3$	$0.083wL^3$
Calculated (Assumption 1)	$0.090wL^3$	$0.088wL^3$	$0.090wL^3$
Calculated (Assumption 2)	$0.093wL^3$	$0.088wL^3$	$0.100wL^3$

Comparison with Total Static Moment.—The total static moment, defined arbitrarily as the sum of the average negative moment plus the total positive moment at midspan, can be calculated for a given bay if the effective position of the vertical reaction is known. The total static moment has been computed on the basis of two assumptions: (1) the shear is uniformly distributed around the column or capital, and (2) the shear is uniformly distributed along all the supported edges including the beams. The results are indicated subsequently. The total static moment should lie between these computed values. The first comparison is made between moments in bays that include the entire structure. In effect, the three-dimensional structure has been reduced to a two-dimensional frame in Table 5.

The second comparison is made between moments in an interior strip of panels or bays one panel in width, such as panels BEH or DEF. In this case, it is necessary to ignore the twisting moments and shears across the interior column center lines (Table 5).

In the first case, the measured moments compare favorably with the range of total static moment computed. The differences are relatively small and may be ascribed partly to the twisting moments. The second comparison is also quite favorable in view of the fact that the assumption of no shears or twisting moments existing along the column center lines is not true for a structure composed mainly of exterior or nonsymmetrical panels. The ideal case, the condition considered by Nichols,[9] is approached in the interior panel of structure F3.

Comparison with Design Moments.—A comparison of the measured and design moments gives an indication of the ability of the design method to provide for the moment. The distribution of measured bending moments is compared with the working stress design moment (ACI 318-63)[10] in Fig. 19. In certain locations, the measured moments exceeded the design moments by as much as 50% at the faces of the interior columns in sections 3 and 5. The measured moment was consistently greater than the design moment across sections 2, 3, 5, and 6.

The measured and design moment coefficients at the various design sections are given in Table 4. These coefficients are compared graphically in Fig. 20. Points falling on the 45° line refer to sections where the measured and design moments were equal. The wall strips and beams were consistently overdesigned, whereas the columns and middle strips were underdesigned.

In view of the differences between measured and design moments at the design strips, a comparison between the moments across the entire structure is given subsequently.

For the sections in panels adjacent and parallel to the shallow beam:

	Section 1	Section 2	Section 3 (exterior)
Measured	$0.085\ wL^3$	$0.145\ wL^3$	$0.236\ wL^3$
Design	$0.130\ wL^3$	$0.125\ wL^3$	$0.188\ wL^3$

For the interior panel sections:

	Section 3 (interior)	Section 4	Section 5 (interior)
Measured	$0.220\ wL^3$	$0.077\ wL^3$	$0.226\ wL^3$
Design	$0.180\ wL^3$	$0.095\ wL^3$	$0.180\ wL^3$

For the sections in panels adjacent and parallel to the deep beams:

	Section 5 (exterior)	Section 6	Section 7
Measured	$0.241\ wL^3$	$0.146\ wL^3$	$0.088\ wL^3$
Design	$0.188\ wL^3$	$0.125\ wL^3$	$0.126\ wL^3$

9 Nichols, J. R., "Statical Limitations Upon the Steel Requirement in Reinforced Concrete Flat Slab Floors," Transactions, ASCE, Vol. 77, 1914, pp. 1670-1736.

10 "Building Code Requirements for Reinforced Concrete (ACI 318-63)," ACI Committee 318, ACI Standard, Amer. Concrete Inst., Detroit, 1963.

It is interesting to note that only in sections 1, 4, and 7 where the design moments greater than the measured moments. The relative difference between the measured and design moments in the remaining sections is not necessarily serious if the capacity of the overdesigned sections can be developed.

FLEXURAL STRENGTH

Calculation of Flexural Strength.—The flexural strength was determined for two possible collapse mechanisms. Mechanism 1 is a slab failure shown in Fig.

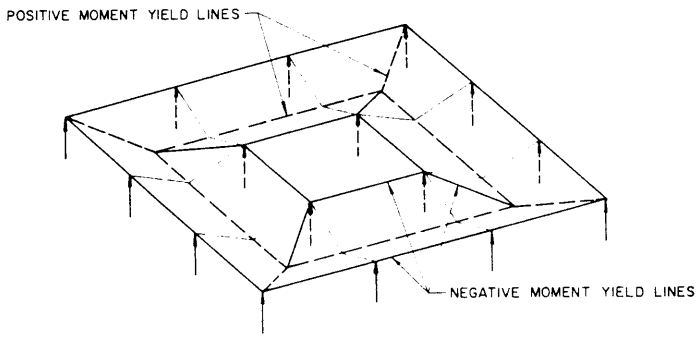

FIG. 21.—FAILURE MECHANISM 1

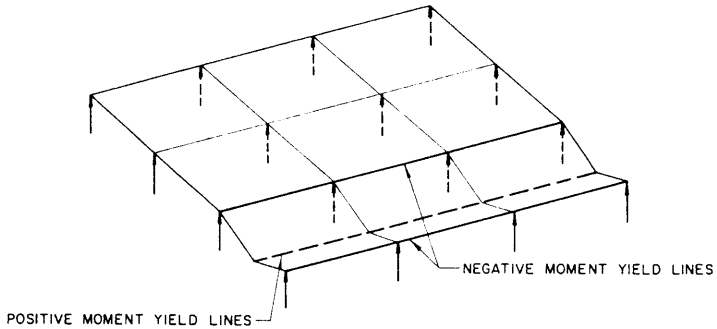

FIG. 22.—FAILURE MECHANISM 2

21. It is assumed that the beams do not participate in the failure. Mechanism 2 (Fig. 22) is a structural failure in that the yield lines cross the entire structure including the beams. Such a mechanism may form in any of the bays of the structure.

The moments across the sections at which yield lines formed were computed using the straight-line formula,

$$M = A_s f_s j d \quad \ldots\ldots\ldots\ldots\ldots\ldots (1)$$

Two values of steel stress were used; the 0.2% offset stress and the ultimate stress. However, it is unlikely that the ultimate stress could actually be attained because it is impossible for the steel at all sections to reach this value. Once the steel reaches ultimate stress, it has little ductility and fracture follows immediately, thereby preventing remaining sections from developing fully. The moment capacity at ultimate stress computed using the formula

$$M_u = A_s f_{su} d (1-0.4 p f_y/f_{cu}) \quad \ldots\ldots\ldots\ldots\ldots (2)$$

gave essentially the same flexural strength.

The yield moment was used in determining the strength of the spandrel beams; the beam reinforcement had a well-defined yield point. The deep beams were assumed to be L-beams with a flange width equal to the width of the beam plus four slab thicknesses.

TABLE 7

Failure Mode	Calculated Flexural Strength Capacity, in pounds per square feet	
	0.2% Offset stress	Ultimate Stress
Mechanism 1:		
Row of panels adjacent to shallow beam	875	965
Row of panels adjacent to deep beams	775	875
Mechanism 2:		
Row of panels adjacent to shallow beams	1040	1090
Row of panels adjacent to deep beams	970	1030

The vertical shear was assumed to be distributed uniformly along all the supported edges including the beams. The slab was considered to rotate freely about the effective position of the vertical reaction except for the resistance of the flexural moments. Twisting moments and planar forces were ignored.

Comparison of Calculated and Measured Strength.—The calculated flexural strength for the two collapse mechanisms and two values of steel stress are summarized in Table 7.

A comparison of these results shows that the critical mechanism should be a slab failure (mechanism 1) in the panels adjacent to the deep beam. The crack patterns of the structure following failure indicated that the yield lines for Mechanism 1 were formed except at the faces of the spandrel beams. The hinging action at the edge of the structure was centered in the beam-column connection which underwent considerable rotation as the beam twisted with respect to the column. The moments at the faces of the beams were well below yielding.

The measured ultimate load of 955 psf exceeds the computed value by approximately 10%. Failure occurred in the panels adjacent to the shallow beam.

However, as was pointed out previously, failure was imminent in all edge panels. In addition, the assumption of a uniform shear distribution along all supported edges established the effective center of reaction closer to the edge of the structure at the deep beam edge and gave a conservative estimate of the strength. It is likely that the effective center of reaction was nearly the same at the shallow and deep beam edges. It is also important to remember that planar forces were ignored and a higher strength would have been computed if these forces had been considered. Planar forces were undoubtedly exerted by the elements of the structure and restrained the deformations of the mechanism.

GENERAL REMARKS

The "empirical method" of design for flat slabs has resulted in successful structures as evidenced by its long and widespread use. Its over-all success has hidden certain weaknesses and limitations of the method.

The empirical method is based on an incorrect definition of the static moment in an interior panel.[4] The total static moment in any portion of the structure has to abide by conditions of equilibrium, and does. The experimental results from the other two flat slabs tested in this series (F1 and F2)[5,6] and the results of F3 corroborate Nichols' analysis.[9]

Designing for a moment less than that obtained from conditions of statics can be defended on the basis of the uncertainties in loading magnitudes and patterns. However, the satisfactory behavior of the structure, even under the assumed design loads, is due primarily to the contribution of concrete tensile strength to slab stiffness at working loads and to the redistribution of moments within the structure. The redistribution allows the overstrength of the peripheral panels to compensate for the understrength of the interior panels.

An obvious limitation of the empirical method (ACI 318-56) is underscored by the comparison of the measured factors of safety for structures F2 and F3. Both structures were designed for a working stress of 20 ksi. Intermediate grade steel was used in structure F2 whereas high strength steel was used in F3. Consequently, the measured over-all factors of safety were 1.9 for F2 and 3.4 for F3. Such discrepancy is unnecessary and avoidable even within the framework of a working-stress method for design. Working stresses for high strength steel can be raised with due attention to requirements of serviceability.

The low deflections of structure F3 relative to those of F2 under the design load are to be attributed to the quality of the concrete. At that level of loading the reinforcement stresses are low, and it makes no difference what the yeild stress of the steel is, provided the yield stress is greater than the steel stresses existing in the structure. However, the quality of the concrete is important because general cracking changes the stiffness of the slab appreciably.[11]

On the other hand, the smaller deflections of F3 relative to those of F2 at loads approaching the failure load of F2 were due primarily to the use of welded wire fabric, which had a high yield stress, in F3.

[11] Vanderbilt, M. D., Sozen, M. A., and Siess, C. P., "Deflections of Multiple-Panel Reinforced Concrete Floor Slabs," Journal of the Structural Division, ASCE, Vol. 91, No. ST4, Proc. Paper 4439, August, 1965, pp. 77-101.

While both F1[5] and F2[6] developed cracks, along yield lines, of considerable width well in advance of failure, the cracks along the yield lines in F3 were on the order of 0.01 in. at loads approaching failure. One reason for the small crack widths at significant overloads was that the slab reinforcement did not exhibit a yield range (Fig. 6). Furthermore, the welded transverse wires caused a large number of cracks with a corresponding decrease in crack width. However, the low ductility of the high-strength steel resulted in the abrupt fracture of the yield line.

As in the cases of F1 and F2, the ultimate load test of F3 emphasized that a major problem in the design of slabs is the transfer of the load from slab to supporting members. For example, although reinforcement is provided to transfer moment from the slab to the spandrel beams, no provision is made to transfer this moment from the beams to the columns. In structure F3, the negative moment reinforcement anchored in the beams was virtually wasted because the beam-column connection did not have sufficient torsional strength. The designer must devote more attention to details of connections between the slab and the columns, wall, or beams than is done generally.

In conclusion, it should be pointed out that what should have been the strength of the empirical method, its simplicity and flexibility as originally conceived, has been overshadowed by the gradual development of rigid requirements that stifle the designer. As shown by test and theory, the limitations placed on the empirical method can be relaxed, leading to versatility and economy.

SUMMARY AND CONCLUSIONS

This paper describes the behavior, at various stages of loading, of a flat slab reinforced with welded wire fabric. The test structure was one of five built and tested in an investigation to develop a unified design approach for all types of reinforced concrete floor slabs.[4]

The structure shown in Figs. 1 and 2 was designed on the basis of the "empirical design method" of ACI 318-56.[7] The total design load for the slab was 285 psf. Reinforcement details are given in Figs. 3 through 5.

The test structure was loaded at 16 points in each of its nine panels to simulate a uniform load. A series of tests was conducted at different load levels and with different combinations of loaded panels. The results of three major tests are examined herein.

Representative load-deflection curves are presented in Fig. 7. Distribution of deflections at various load levels are shown in Figs. 8, 11, and 14. The distribution of steel stress across different sections (Fig. 1) are given in Figs. 9 and 10 for five levels of loading.

At working load, the behavior of the structure was characterized by small deflections and stresses. This was primarily due to the contribution of concrete tensile strength to flexural resistance. The structure was essentially uncracked after reaching design load. Under increased loading, the stresses and deflections increased at an increasing rate as cracking progressed. The load was steadily increased to 955 psf when failure occurred. Failure was marked by fracture of the positive moment reinforcement in panels A and B.

The bending moments at the various design sections were evaluated using strains measured under design load (Test 502) and a moment-strain relation-

ship shown in Fig. 18. The computed unit moments are compared with design unit moments in Fig. 19. Computed and design moments across the design sections are compared in Table 4. The structure, considered in its entirety, was adequately designed as shown by the comparisons. However, the distribution of reinforcement as dictated by the empirical method was inefficient.

Studies of the behavior and strength of the test structure indicate that high-strength steel can be used efficiently in flat slabs, provided that serviceability criteria are satisfied explicitly and that the empirical method of design can be modified to become simpler and more general.

ACKNOWLEDGMENTS

This paper is based on an investigation conducted in the Structural Research Laboratory of the University of Illinois Civil Engineering Department. Contributions in support of the project were received from the following organizations: Reinforced Concrete Research Council; Engineering Foundation; Concrete Reinforcing Steel Institute; Portland Cement Association; Wire Reinforcement Institute; Directorate of Civil Engineering, Headquarters, U.S. Air Force; General Services Administration, Public Buildings Service; Office of the Chief of Engineers, Corps of Engineers, U.S. Army; and Bureau of Yards and Docks, Engineering Division, U. S. Navy.

The project was initiated by the Joint ACI-ASCE Committee on Design of Reinforced Concrete Slabs and was guided by an advisory committee on which the following persons have served: L. H. Corning (Chairman 1956-1962), Douglas McHenry (present Chairman), G. B. Begg, Jr., W. J. Bobisch, F. B. Brown, M. P. van Buren, A. S. Neiman, N. M. Newmark, D. H. Pletta, J. R. Powers, Paul Rogers, E. J. Ruble, W. E. Schaem, Joseph DiStasio, Sr., A. I. Westrich, and C. A. Willson.

The prototype design was made by the firm of DiStasio and van Buren, Consulting Engineers, New York, N. Y., with the personal attention of M. P. van Buren.

The dedicated help of E J. Strougal in the construction, instrumentation, and testing of structure F3 is gratefully acknowledged. Much of the routine of data recording and reduction was eliminated through the resourcefulness of V. J. McDonald.

Acknowledgment is due D. S. Hatcher, W. G. Corley, W. L. Gamble, and M. D. Vanderbilt whose parallel studies have been used in or have influenced this paper.